

Supplementary Information

Towards an understanding of photoluminescence in lead-free $\text{Cs}_2\text{Ag}_x\text{Na}_{1-x}\text{Bi}_y\text{In}_{1-y}\text{Cl}_6$ double perovskites by machine learning prediction from density-functional theory ground state properties

Marina S. Günthert^{1,2}, Larry Lüer¹, Oleksandr Stroyuk³, Oleksandra Raievska³,
Christian Kupfer^{1,3}, Andres Osvet¹, Bernd Meyer², Christoph J. Brabec^{1,3,4}

¹ Friedrich-Alexander-Universität Erlangen-Nürnberg,
Materials for Electronics and Energy Technology (i-MEET),
91058 Erlangen, Germany

² Friedrich-Alexander-Universität Erlangen-Nürnberg,
Interdisciplinary Center for Molecular Materials (ICMM) and Computer Chemistry Center (CCC),
91052 Erlangen, Germany

³ Forschungszentrum Jülich GmbH,
Helmholtz-Institut Erlangen-Nürnberg für Erneuerbare Energien (HI ERN),
91058 Erlangen, Germany

⁴ Forschungszentrum Jülich GmbH,
Institute of Energy Technologies (IET), Institute of Energy Materials and Devices (IMD), Photovoltaic (IMD-3),
52428 Jülich, Germany

Email:

marina.guenthert@fau.de
bernd.meyer@fau.de
christoph.brabec@fau.de

	Cs		Ag		Na		Bi		In		Cl	
	nom	exp	nom	exp	nom	exp	nom	exp	nom	exp	nom	exp
A 1	20	22.45	0	0.00	10	6.90	0	0.05	10	10.80	60	59.75
A 2	20	22.20	0	0.00	10	7.65	1	0.70	10	10.25	60	59.20
A 4	20	23.58	0	0.00	10	4.90	3	4.30	8	9.08	60	59.70
A 5	20	20.95	0	0.00	10	11.05	5	6.80	5	4.00	60	57.23
A 6	20	21.76	0	0.00	10	10.28	8	8.92	3	1.76	60	57.30
A 7	20	21.38	0	0.00	10	9.48	9	10.18	1	0.78	60	58.20
A 8	20	21.80	0	0.00	10	8.83	10	11.75	0	0.05	60	57.55
B 1	20	23.78	1	0.58	9	5.53	0	0.08	10	11.50	60	58.55
B 2	20	21.45	1	1.35	9	9.18	1	0.48	10	9.98	60	56.75
B 3	20	22.60	1	0.65	9	6.70	1	1.03	9	10.60	60	58.45
B 4	20	23.03	1	1.00	9	5.35	3	3.15	8	8.30	60	59.10
B 5	20	27.30	1	1.02	9	5.66	5	6.76	5	3.46	60	55.82
B 6	20	20.93	1	1.43	9	9.60	8	9.28	3	1.10	60	57.63
B 7	20	23.06	1	0.94	9	9.00	9	10.38	1	0.66	60	55.96
B 8	20	22.00	1	1.28	9	8.60	10	11.00	0	0.00	60	57.13
C 1	20	21.92	3	2.68	7	7.00	0	0.02	10	10.10	60	58.20
C 2	20	21.75	3	3.30	7	6.78	1	0.60	10	9.38	60	58.18
C 3	20	20.65	3	3.18	7	7.98	1	1.20	9	9.03	60	57.93
C 4	20	21.98	3	3.53	7	5.15	3	2.83	8	7.50	60	58.98
C 5	20	21.93	3	3.68	7	6.35	5	6.53	5	4.03	60	57.43
C 6	20	22.33	3	3.28	7	7.80	8	8.45	3	2.08	60	56.10
C 7	20	21.70	3	3.53	7	6.18	9	10.10	1	0.68	60	57.83
C 8	20	20.58	3	3.48	7	8.15	10	10.85	0	0.08	60	56.78
D 1	20	22.54	5	4.76	5	4.02	0	0.08	10	10.20	60	58.04
D 2	20	20.00	5	5.45	5	7.40	1	0.65	10	9.25	60	57.28
D 3	20	20.08	5	5.40	5	7.90	1	1.13	9	8.93	60	56.55
D 4	20	20.36	5	5.16	5	6.82	3	2.84	8	7.40	60	57.42
D 5	20	20.64	5	5.28	5	6.96	5	5.22	5	5.10	60	56.62
D 6	20	21.33	5	5.55	5	6.55	8	8.43	3	2.38	60	56.40
D 7	20	21.23	5	5.10	5	5.45	9	9.98	1	0.90	60	57.40
D 8	20	22.05	5	5.13	5	5.55	10	11.28	0	0	60	56.05
E 1	20	21.43	8	6.23	2	3.15	0	0.15	10	10.10	60	58.93
E 2	20	20.65	8	7.05	2	4.93	1	0.55	10	9.25	60	57.55
E 3	20	21.45	8	6.88	2	3.70	1	1.08	9	8.98	60	57.95
E 4	20	22.35	8	6.98	2	2.10	3	2.83	8	7.28	60	58.43
E 5	20	21.08	8	8.84	2	2.36	5	5.52	5	4.84	60	57.40
E 6	20	20.90	8	9.40	2	2.10	8	8.80	3	1.95	60	56.83
E 7	20	20.50	8	9.08	2	3.00	9	10.23	1	0.58	60	56.65
E 8	20	20.70	8	8.66	2	3.16	10	10.62	0	0.06	60	56.80
F 1	20	20.28	10	5.75	0	5.60	0	0.15	10	9.53	60	58.73
F 2	20	20.08	10	7.35	0	5.10	1	0.50	10	9.23	60	57.75
F 3	20	21.55	10	7.33	0	3.33	1	1.00	9	8.60	60	58.20
F 4	20	20.03	10	9.35	0	3.58	3	2.58	8	7.20	60	57.28
F 5	20	21.75	10	9.28	0	1.10	5	5.78	5	4.43	60	57.63
F 6	20	20.75	10	10.53	0	1.58	8	8.68	3	1.80	60	56.75
F 7	20	20.58	10	10.80	0	1.20	9	10.36	1	0.40	60	56.60
F 8	20	20.28	10	10.70	0.00	1.35	10	10.60	0	0.05	60	57.03

Table S1: EDX results for CANBIC (in at%)

	In %								
	0	12.5	25	37.5	50	62.5	75	87.5	100
0	10.67	10.63	10.60	10.56	10.53	10.49	10.46	10.42	10.39
12.5	10.69	10.65	10.62	10.58	10.55	10.51	10.47	10.43	10.40
25	10.70	10.66	10.63	10.59	10.56	10.52	10.48	10.44	10.41
37.5	10.72	10.68	10.65	10.61	10.58	10.53	10.50	10.46	10.42
Na % 50	10.73	10.69	10.66	10.62	10.59	10.55	10.51	10.47	10.44
62.5	10.75	10.71	10.68	10.64	10.61	10.57	10.53	10.49	10.45
75	10.76	10.73	10.69	10.66	10.62	10.58	10.55	10.50	10.47
87.5	10.79	10.75	10.72	10.68	10.64	10.60	10.56	10.52	10.48
100	10.81	10.77	10.73	10.69	10.66	10.62	10.58	10.54	10.50

Table S2: DFT computed CANBIC lattice parameter (in Å)

	In %								
	0	12.5	25	37.5	50	62.5	75	87.5	100
0	31.86	31.01	30.46	30.51	30.77	31.13	31.85	31.91	31.58
12.5	29.68	28.98	29.19	28.55	28.81	29.22	29.65	30.16	30.71
25	28.63	28.19	27.96	27.25	27.49	27.65	28.24	28.97	29.10
37.5	26.26	26.26	26.29	26.19	25.71	25.86	26.57	26.97	27.68
Na % 50	25.40	25.34	25.74	25.20	24.51	24.63	25.08	25.62	26.62
62.5	23.40	23.07	23.88	23.88	24.02	23.09	23.42	23.94	25.06
75	21.49	22.17	23.18	23.31	23.55	22.15	22.44	22.85	23.68
87.5	20.32	21.21	21.22	21.21	22.40	21.59	21.28	21.44	22.45
100	17.92	19.35	20.74	21.15	21.83	21.34	20.49	20.76	21.33

Table S3: DFT computed CANBIC bulk modulus (in GPa)

	In %								
	0	12.5	25	37.5	50	62.5	75	87.5	100
0	20.24	19.91	19.62	19.53	19.47	19.08	18.73	18.09	17.50
12.5	20.06	19.90	19.76	19.51	19.29	18.96	18.66	18.04	17.37
25	20.18	20.13	19.90	19.56	19.10	18.93	18.66	17.97	17.48
37.5	20.24	19.99	19.70	19.30	18.95	18.77	18.45	18.01	17.40
Na % 50	20.39	19.89	19.58	19.21	18.84	18.54	18.23	17.84	17.33
62.5	20.50	19.97	19.58	19.20	18.82	18.55	18.35	17.84	17.14
75	20.51	20.10	19.73	19.37	18.97	18.66	18.35	17.80	17.33
87.5	20.61	20.27	19.78	19.30	18.93	18.57	18.20	17.74	17.25
100	20.74	20.16	19.86	19.26	18.97	18.53	18.07	17.64	17.14

Table S4: DFT computed CANBIC shear modulus (in GPa)

		In %								
		0	12.5	25	37.5	50	62.5	75	87.5	100
Na %	0	0.24	0.24	0.23	0.24	0.24	0.25	0.25	0.26	0.27
	12.5	0.22	0.22	0.22	0.22	0.23	0.23	0.24	0.25	0.26
	25	0.21	0.21	0.21	0.21	0.22	0.22	0.23	0.24	0.25
	37.5	0.19	0.20	0.20	0.20	0.20	0.21	0.22	0.23	0.24
	50	0.18	0.19	0.20	0.20	0.19	0.20	0.21	0.22	0.23
	62.5	0.16	0.16	0.18	0.18	0.19	0.18	0.19	0.20	0.22
	75	0.14	0.15	0.17	0.17	0.18	0.17	0.18	0.19	0.21
	87.5	0.12	0.14	0.14	0.15	0.17	0.17	0.17	0.18	0.19
	100	0.08	0.11	0.14	0.15	0.16	0.16	0.16	0.17	0.18

Table S5: DFT computed CANBIC Poisson ratio

		In %								
		0	12.5	25	37.5	50	62.5	75	87.5	100
Na %	0	227.94	227.32	227.05	227.89	229.00	228.22	227.82	225.57	223.47
	12.5	228.30	228.57	229.27	229.16	229.40	229.00	228.86	226.76	224.32
	25	230.40	231.41	231.52	230.94	229.85	230.38	230.44	227.99	226.61
	37.5	232.03	232.06	231.92	231.04	230.46	230.97	230.79	229.74	227.79
	50	234.38	233.07	232.91	232.18	231.46	231.22	231.06	230.37	229.10
	62.5	236.35	234.86	234.43	233.77	233.14	232.89	233.37	232.00	229.55
	75	237.75	237.22	236.98	236.53	235.85	235.26	235.15	233.52	232.48
	87.5	239.99	239.93	238.82	237.58	237.43	236.65	236.04	234.84	233.79
	100	241.90	240.73	241.12	239.38	239.55	238.48	237.17	236.19	235.00

Table S6: DFT computed CANBIC Debye temperature (in K)

		In %								
		0	12.5	25	37.5	50	62.5	75	87.5	100
Na %	0	3.49	2.53	2.59	2.41	2.35	2.23	1.98	2.29	2.41
	12.5	2.65	2.59	2.71	2.53	2.41	2.29	2.05	2.65	2.53
	25	2.65	2.65	2.41	2.59	2.53	2.41	2.29	2.77	2.71
	37.5	2.71	2.71	2.65	2.77	2.65	2.53	2.29	2.95	2.89
	50	2.71	2.77	2.71	2.83	2.65	2.77	2.89	3.07	3.25
	62.5	2.77	2.89	2.77	3.01	2.89	3.07	3.31	3.19	3.25
	75	2.77	2.83	2.77	2.95	2.83	3.19	3.43	3.37	3.31
	87.5	3.43	3.43	3.37	3.43	3.43	3.37	3.49	3.43	3.43
	100	3.97	3.97	4.09	4.15	3.67	4.09	4.03	4.15	4.15

Table S7: DFT computed CANBIC absorption onset (in eV)

	In %									
	0	12.5	25	37.5	50	62.5	75	87.5	100	
0	1.58	1.58	1.50	1.29	1.13	1.62	1.85	1.19	0.79	
12.5	1.58	1.76	1.61	1.45	1.26	1.70	1.88	1.29	0.93	
25	1.57	1.84	1.69	1.55	1.36	1.75	1.90	1.42	1.09	
37.5	1.65	1.85	1.73	1.74	1.56	1.83	1.98	1.57	1.24	
Na % 50	1.69	1.85	1.76	1.87	1.70	1.87	1.98	1.70	1.42	
62.5	1.80	1.93	2.03	2.09	1.98	2.13	2.10	1.92	1.68	
75	1.87	1.96	2.06	2.20	2.23	2.32	2.36	2.22	2.07	
87.5	2.59	2.61	2.63	2.61	2.62	2.57	2.62	2.47	2.32	
100	3.67	3.49	3.48	3.34	3.26	3.16	3.19	2.99	3.08	

Table S8: DFT computed CANBIC bandgap (in eV)

	In %									
	0	12.5	25	37.5	50	62.5	75	87.5	100	
0	5.06	5.03	5.13	5.40	5.60	5.63	5.76	6.32	6.79	
12.5	5.04	5.00	5.13	5.35	5.57	5.61	5.63	6.24	6.72	
25	5.04	5.03	5.15	5.34	5.60	5.57	5.62	6.12	6.54	
37.5	5.04	5.00	5.14	5.36	5.54	5.57	5.59	6.03	6.40	
Na % 50	5.07	5.01	5.16	5.34	5.60	5.58	5.60	5.91	6.24	
62.5	5.05	5.01	5.09	5.21	5.41	5.39	5.55	5.81	6.08	
75	5.10	5.01	5.12	5.11	5.31	5.34	5.51	5.70	5.91	
87.5	4.63	4.65	4.76	4.91	2.74	2.76	5.34	5.56	3.24	
100	4.18	4.45	4.53	4.71	2.73	2.70	2.71	2.71	2.71	

Table S9: DFT computed CANBIC valence band width (in eV)

	In %									
	0	12.5	25	37.5	50	62.5	75	87.5	100	
0	0.00	0.00	0.01	-0.01	-0.03	-0.43	-0.71	-0.75	-0.79	
12.5	-0.01	-0.10	-0.10	-0.10	-0.10	-0.47	-0.71	-0.74	-0.78	
25	-0.01	-0.16	-0.18	-0.17	-0.17	-0.49	-0.71	-0.74	-0.77	
37.5	-0.08	-0.16	-0.18	-0.29	-0.32	-0.54	-0.72	-0.78	-0.78	
Na % 50	-0.09	-0.14	-0.18	-0.38	-0.41	-0.56	-0.71	-0.78	-0.78	
62.5	-0.15	-0.20	-0.22	-0.45	-0.52	-0.68	-0.84	-0.91	-0.91	
75	-0.22	-0.23	-0.24	-0.46	-0.65	-0.82	-1.08	-1.10	-1.12	
87.5	-0.48	-0.48	-0.48	-0.64	-0.78	-0.91	-1.16	-1.18	-1.21	
100	-1.04	-1.08	-1.11	-1.16	-1.19	-1.27	-1.44	-1.46	-1.75	

Table S10: DFT computed CANBIC valence band shift (in eV)

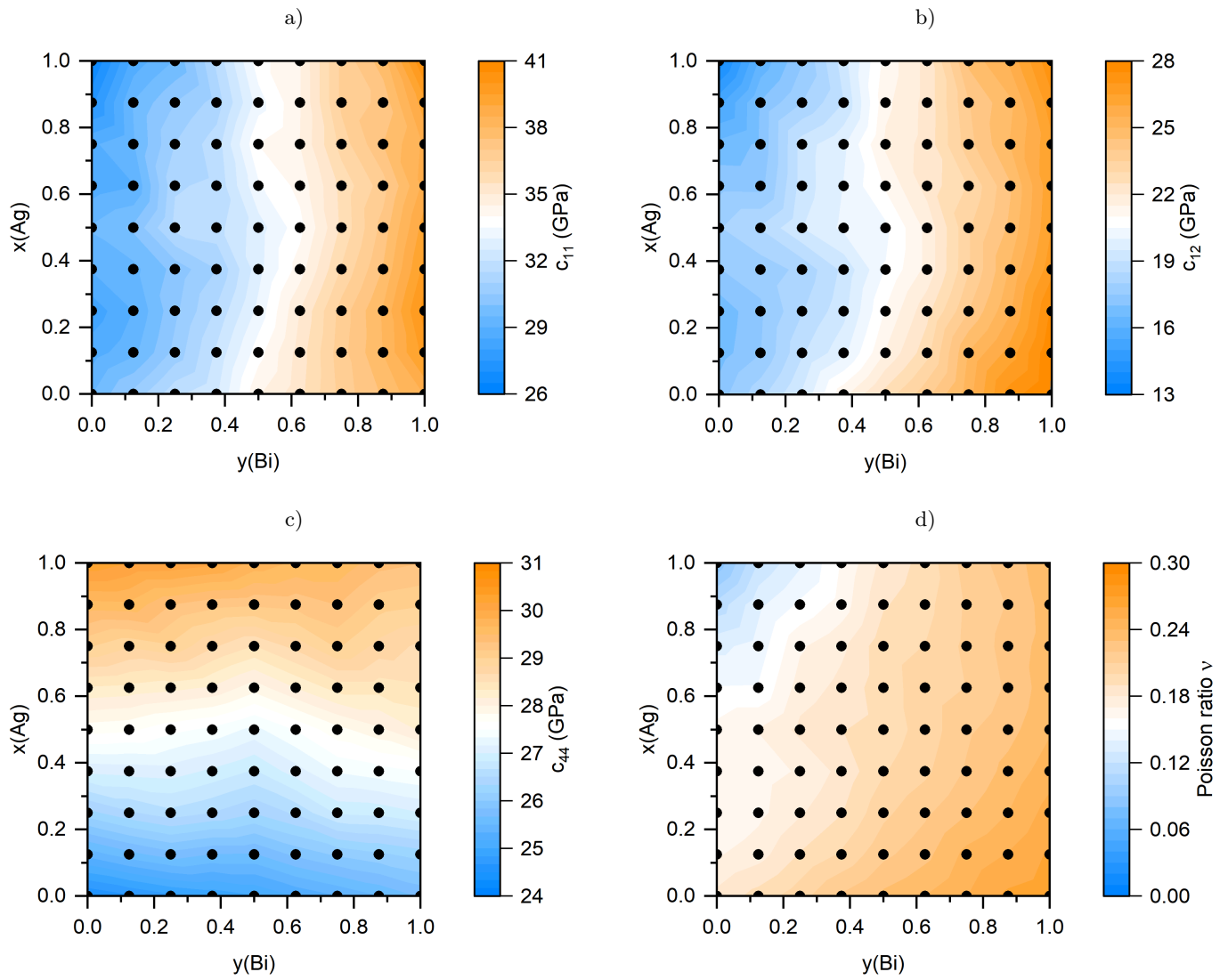


Figure S1: 2D maps of elastic constants of CANBIC (a) c_{11} , (b) c_{12} , (c) c_{44} , (d) Poisson ratio ν

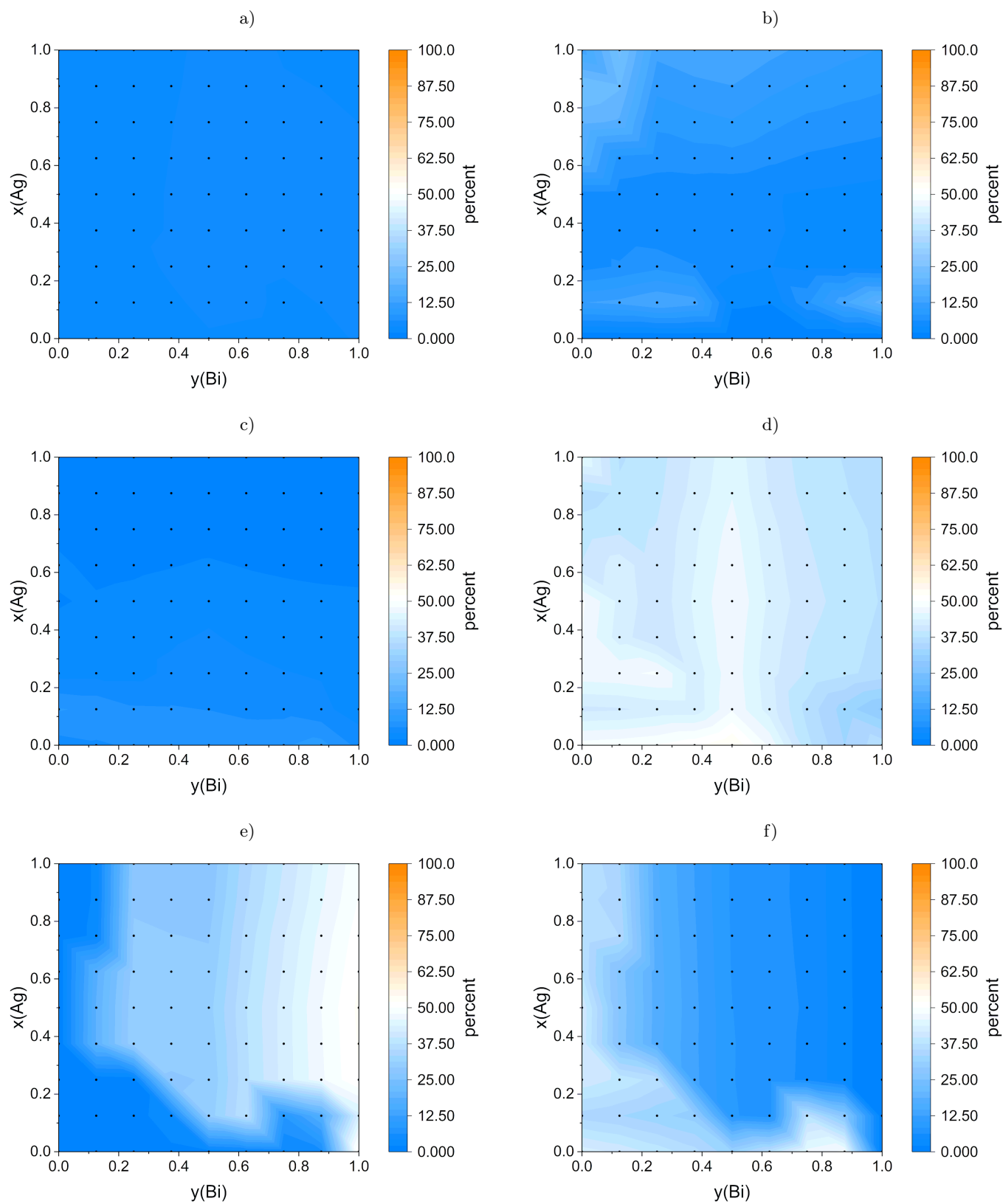


Figure S2: CB fractions in percent (a) Cs, (b) Ag, (c) Na, (d) Cl, (e) Bi, (f) In

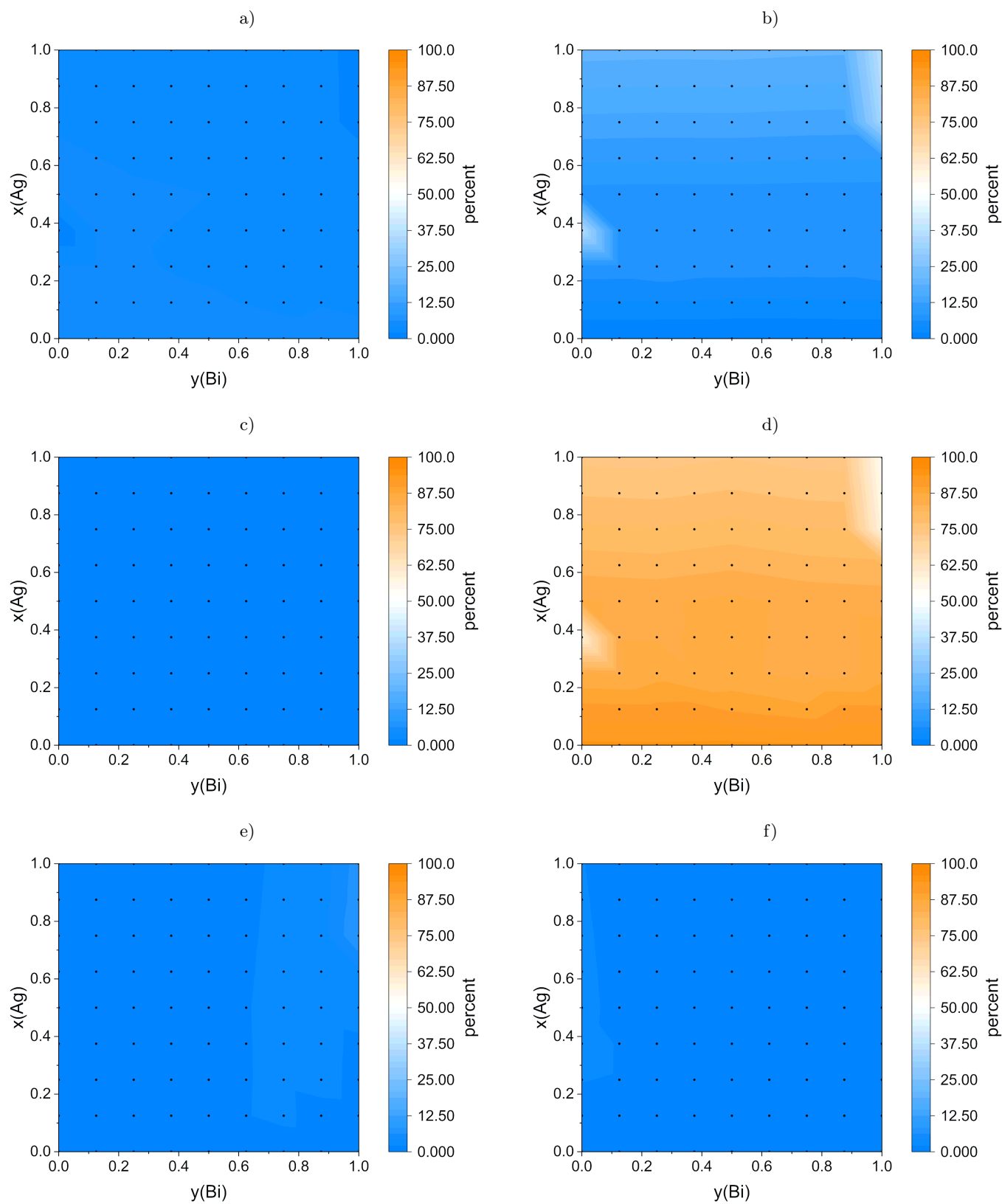


Figure S3: VB fractions in percent (a) Cs, (b) Ag, (c) Na, (d) Cl, (e) Bi, (f) In

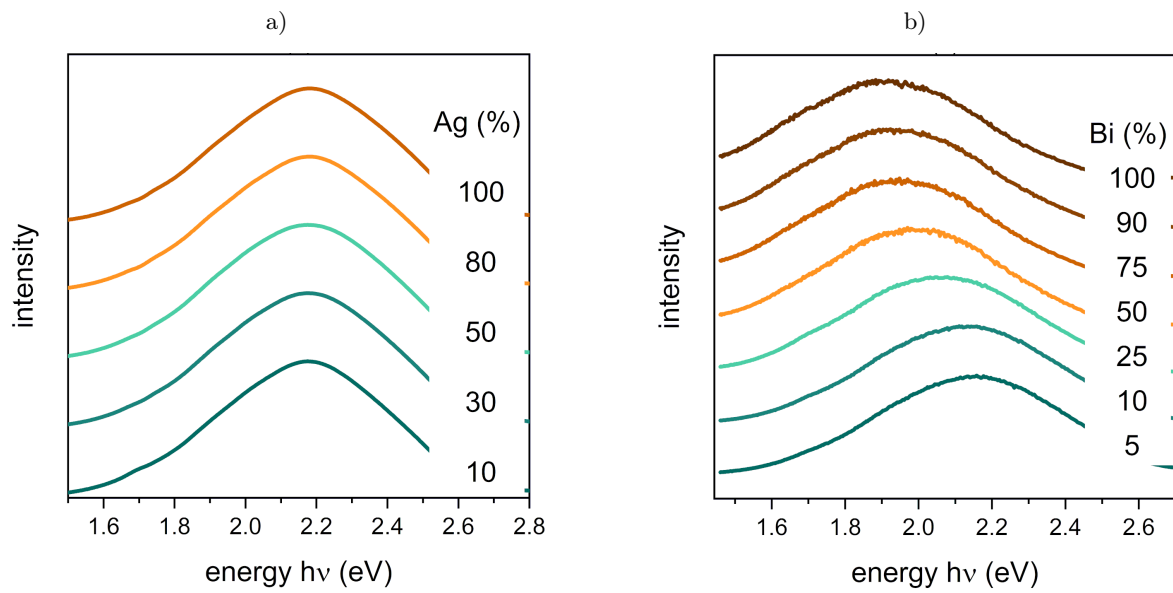


Figure S4: PL spectra of samples (a) with varying Ag content ($\text{Bi} = 0.5$) and (b) with varying Bi content ($\text{Ag} = 0.5$)

Θ_D	$\log(k_{nr})$		VB_{shift}	$\log(k_r)$		ρ	E_s	
	M	$\log(k_{nr})$		Θ_D	$\log(k_r)$		c_{12}	E_s
263.63	774.95	2.30	-0.69	263.63	0.00	0.63	24.63	0.77
264.69	764.34	1.84	-0.54	264.69	-0.61	0.62	22.16	0.83
266.15	753.73	1.25	-0.26	266.15	-0.59	0.61	21.19	0.89
265.69	743.12	1.05	-0.15	265.69	-0.64	0.60	19.29	0.95
265.80	732.51	0.87	-0.11	265.80	-0.50	0.59	17.46	1.02
263.67	721.90	0.86	-0.06	263.67	-0.63	0.57	16.14	1.11
265.50	763.06	2.10	-0.71	265.50	-0.63	0.63	23.97	0.78
265.25	752.45	1.67	-0.59	265.25	-0.76	0.62	22.16	0.83
265.81	741.84	1.07	-0.32	265.81	-0.65	0.61	21.37	0.88
265.80	731.23	0.96	-0.21	265.80	-0.67	0.59	19.01	0.94
266.06	720.62	0.81	-0.18	266.06	-0.56	0.58	18.01	1.01
264.33	710.01	0.57	-0.09	264.33	-0.57	0.57	17.04	1.10
267.40	751.16	1.67	-0.78	267.40	-0.64	0.63	23.83	0.79
266.61	740.55	1.50	-0.63	266.61	-0.54	0.61	22.18	0.84
265.81	729.94	1.15	-0.44	265.81	-0.53	0.60	21.60	0.89
266.63	719.33	0.82	-0.36	266.63	-0.54	0.59	19.93	0.95
267.20	708.72	0.47	-0.22	267.20	-0.71	0.58	19.27	1.01
265.25	698.11	0.30	-0.21	265.25	-0.56	0.57	17.10	1.08
267.13	739.27	1.29	-0.79	267.13	-0.52	0.62	23.05	0.82
266.36	728.66	1.16	-0.65	266.36	-0.49	0.61	22.20	0.85
265.69	718.05	1.03	-0.51	265.69	-0.44	0.60	21.08	0.89
266.48	707.44	0.67	-0.44	266.48	-0.44	0.59	20.02	0.95
266.91	696.83	0.31	-0.29	266.91	-0.58	0.58	19.25	1.01
266.24	686.22	0.14	-0.22	266.24	-0.57	0.56	17.33	1.06
268.06	727.37	0.98	-0.93	268.06	-0.39	0.62	23.44	0.85
267.18	716.76	0.74	-0.77	267.18	-0.46	0.61	21.64	0.87
267.24	706.15	0.77	-0.62	267.24	-0.41	0.59	20.38	0.90
267.26	695.54	0.48	-0.55	267.26	-0.38	0.58	20.12	0.95
266.57	684.93	0.32	-0.41	266.57	-0.52	0.57	19.49	1.01
266.38	674.32	0.20	-0.31	266.38	-0.59	0.56	18.56	1.05
268.74	715.48	0.66	-1.07	268.74	-0.24	0.61	23.46	0.87
268.26	704.87	0.26	-0.92	268.26	-0.35	0.60	21.66	0.88
267.91	694.26	0.47	-0.75	267.91	-0.34	0.59	20.54	0.92
267.26	683.65	0.26	-0.57	267.26	-0.39	0.58	19.14	0.96
268.18	673.04	0.26	-0.45	268.18	-0.65	0.57	18.14	1.00
267.30	662.43	0.23	-0.35	267.30	-0.63	0.56	17.70	1.02
271.14	703.58	0.21	-1.16	271.14	-0.05	0.61	24.00	0.88
271.96	692.97	-0.06	-1.02	271.96	-0.14	0.60	22.35	0.88
271.63	682.36	0.25	-0.88	271.63	-0.15	0.59	21.05	0.91
269.31	671.75	-0.04	-0.75	269.31	-0.20	0.57	19.34	0.96
269.61	661.14	0.11	-0.66	269.61	-0.37	0.56	18.47	0.99
268.42	650.53	0.21	-0.61	268.42	-0.38	0.55	17.41	0.99
271.95	691.69	-0.36	-1.54	271.95	0.11	0.61	25.04	0.90
271.88	681.07	0.00	-1.39	271.88	0.04	0.60	22.83	0.93
271.75	670.47	-0.04	-1.30	271.75	-0.04	0.58	21.54	0.93
270.61	659.86	-0.51	-1.27	270.61	0.03	0.57	19.86	0.95
269.99	649.25	-0.34	-1.23	269.99	0.01	0.56	18.94	0.98
269.09	638.64	0.11	-1.20	269.09	-0.12	0.55	17.49	0.97

Table S11: ML training data set

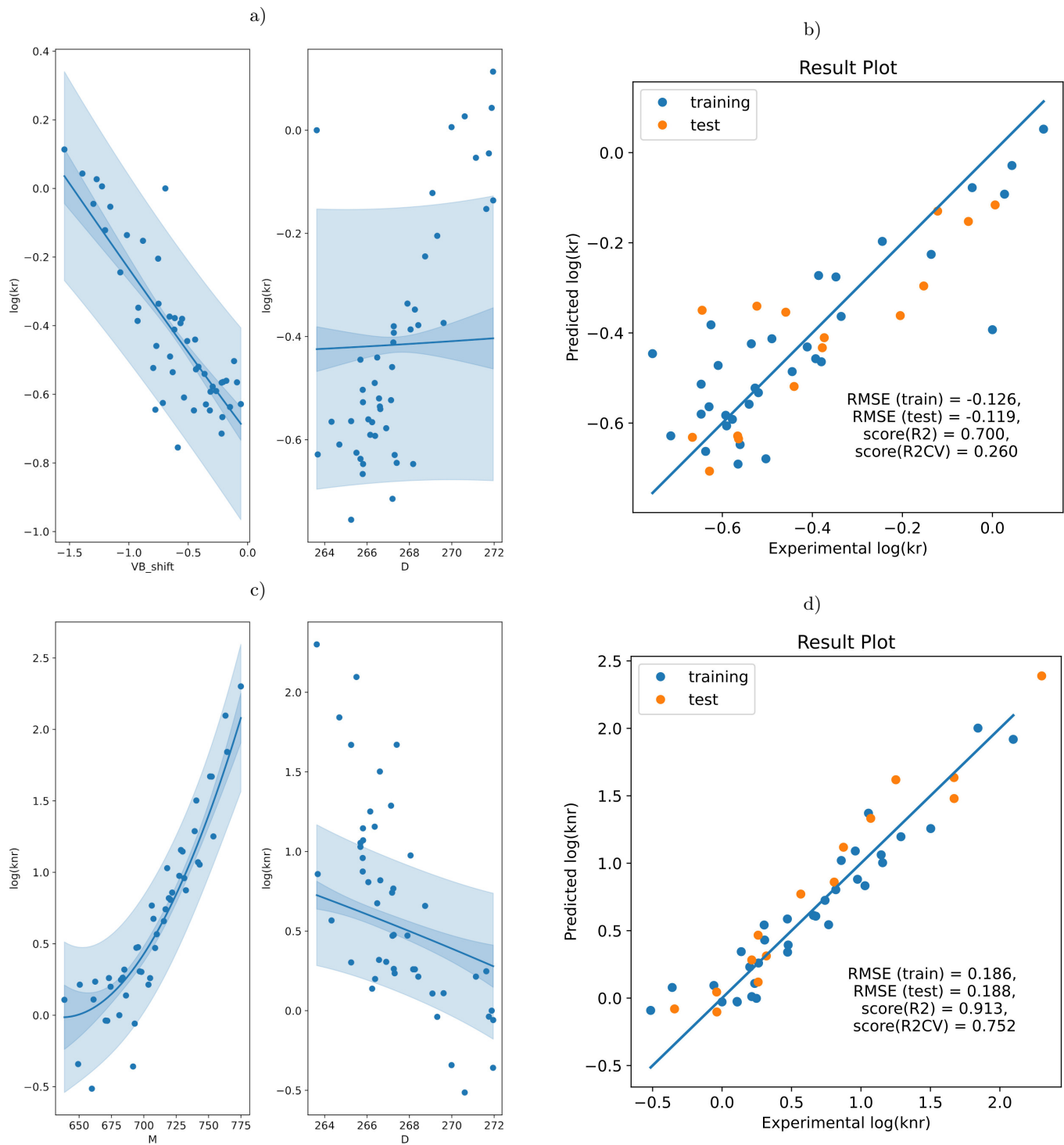


Figure S5: mRMR training data, (a) objective functions for k_r prediction, (b) result plot of k_r prediction, (c) objective functions for k_{nr} prediction, (d) result plot for k_{nr} prediction

		Θ_D									
$\log(k_{nr})$		261.96	263.26	264.55	265.85	267.14	268.44	269.73	271.03	272.33	273.62
M	611.37	0.364	0.291	0.219	0.146	0.073	0.001	-0.072	-0.145	-0.217	-0.290
	632.58	0.312	0.240	0.167	0.094	0.021	-0.052	-0.125	-0.197	-0.270	-0.343
	653.78	0.351	0.278	0.205	0.132	0.060	-0.013	-0.086	-0.159	-0.232	-0.305
	674.99	0.481	0.408	0.335	0.262	0.189	0.116	0.043	-0.030	-0.103	-0.176
	696.19	0.702	0.629	0.556	0.483	0.411	0.338	0.265	0.192	0.119	0.046
	717.39	1.014	0.941	0.868	0.796	0.723	0.650	0.577	0.504	0.431	0.359
	738.60	1.415	1.343	1.270	1.197	1.125	1.052	0.980	0.907	0.834	0.762
	759.80	1.904	1.832	1.760	1.687	1.615	1.543	1.470	1.398	1.326	1.253
	781.01	2.479	2.407	2.335	2.263	2.191	2.119	2.047	1.975	1.903	1.831
	802.21	3.137	3.065	2.994	2.922	2.851	2.779	2.708	2.636	2.564	2.493

Table S12: GPR prediction of $\log(k_{nr})$ from Θ_D (in K) and M (in u)

		VB_{shift}									
$\log(k_r)$		-1.84	-1.61	-1.38	-1.15	-0.92	-0.68	-0.45	-0.22	0.01	0.24
Θ_D	261.96	0.183	0.065	-0.051	-0.165	-0.279	-0.390	-0.498	-0.605	-0.708	-0.808
	263.26	0.183	0.066	-0.051	-0.165	-0.278	-0.390	-0.498	-0.604	-0.708	-0.808
	264.55	0.183	0.066	-0.050	-0.165	-0.278	-0.389	-0.498	-0.604	-0.708	-0.808
	265.85	0.183	0.066	-0.050	-0.165	-0.278	-0.389	-0.498	-0.604	-0.708	-0.808
	267.14	0.183	0.066	-0.050	-0.165	-0.278	-0.389	-0.498	-0.604	-0.707	-0.808
	268.44	0.183	0.066	-0.050	-0.165	-0.278	-0.389	-0.498	-0.604	-0.707	-0.807
	269.73	0.183	0.066	-0.050	-0.165	-0.278	-0.389	-0.498	-0.604	-0.707	-0.807
	271.03	0.183	0.066	-0.050	-0.165	-0.278	-0.389	-0.498	-0.604	-0.707	-0.807
	272.33	0.183	0.066	-0.050	-0.165	-0.278	-0.389	-0.498	-0.604	-0.707	-0.807
	273.62	0.183	0.066	-0.050	-0.165	-0.278	-0.389	-0.498	-0.604	-0.707	-0.807

Table S13: GPR prediction of $\log(k_r)$ from VB_{shift} (in eV) and Θ_D (in K)

		c_{12}									
$\log(k_r)$		14.36	15.75	17.13	18.52	19.90	21.29	22.67	24.05	25.44	26.82
ρ	0.53	1.144	1.121	1.098	1.075	1.051	1.028	1.004	0.980	0.956	0.933
	0.54	1.124	1.101	1.078	1.055	1.032	1.008	0.984	0.960	0.937	0.913
	0.56	1.103	1.080	1.057	1.033	1.010	0.986	0.963	0.939	0.915	0.892
	0.57	1.079	1.057	1.034	1.010	0.987	0.963	0.940	0.916	0.892	0.869
	0.58	1.055	1.032	1.009	0.986	0.962	0.939	0.915	0.892	0.868	0.845
	0.60	1.028	1.005	0.982	0.959	0.936	0.913	0.889	0.866	0.842	0.819
	0.61	1.000	0.978	0.955	0.932	0.909	0.885	0.862	0.839	0.815	0.792
	0.62	0.971	0.948	0.926	0.903	0.880	0.857	0.833	0.810	0.787	0.764
	0.64	0.940	0.918	0.895	0.872	0.850	0.827	0.804	0.781	0.758	0.735
	0.65	0.909	0.886	0.864	0.841	0.818	0.796	0.773	0.750	0.727	0.705

Table S14: GPR prediction of Stokes shift E_s (in eV) from c_{12} (in GPa) and ρ (in u/ \AA^3)